

# Sulfide oxidation and iron dissolution kinetics during the reaction of dissolved sulfide with ferrihydrite

Simon W. Poulton\*

*School of Earth Sciences, University of Leeds, Leeds LS2 9JT, UK*

Received 4 September 2002; accepted 22 July 2003

## Abstract

The reaction between synthetic ferrihydrite and dissolved sulfide was studied in artificial seawater and 0.42 M NaCl at 25 °C over the pH range 4.0–8.2. Electron transfer between solid phase Fe(III) and surface-complexed sulfide results in the reduction of Fe(III) and the formation of elemental sulfur. Subsequent formation of solid phase FeS occurs following dissolution of Fe(II) and reaction with dissolved sulfide. However, the majority of the Fe(II) produced at pH 7.5 remained associated with the oxide surface on the time-scale of these experiments. Rates of both sulfide oxidation and Fe(II) dissolution (in mol l<sup>-1</sup> min<sup>-1</sup>) were expressed in terms of an empirical rate equation of the form:

$$R = k_i(\text{H}_2\text{S})_{t=0}^{0.5} A$$

where  $k_i$  represents the apparent rate constants for the oxidation of sulfide ( $k_S$ ) or the dissolution of Fe<sup>2+</sup> ( $k_{Fe}$ ),  $(\text{H}_2\text{S})_{t=0}$  is the initial sulfide concentration (in mol l<sup>-1</sup>) and  $A$  is the initial ferrihydrite surface area (in m<sup>2</sup> l<sup>-1</sup>). The rate constant,  $k_S$ , for the oxidation of sulfide in seawater at pH 7.5 is  $8.4 \times 10^{-6} \pm 0.9 \times 10^{-6} \text{ mol}^{0.5} \text{ l}^{0.5} \text{ m}^{-2} \text{ min}^{-1}$ , with the rate of sulfide oxidation being approximately 15 times faster than the rate of Fe(II) dissolution (given that the ratio of sulfide oxidized to Fe(II) produced is 2:1;  $k_{Fe} = 1.1 \times 10^{-6} \pm 0.2 \times 10^{-6} \text{ mol}^{0.5} \text{ l}^{0.5} \text{ m}^{-2} \text{ min}^{-1}$ ). The determination of a fractional order with regard to the initial dissolved sulfide concentration occurs because reaction rates are dependent on the availability of reactive surface sites; the more reactive surface sites become saturated with sulfide at relatively low ferrihydrite to dissolved sulfide ratios. In many natural sulfidic environments, the iron oxide to dissolved sulfide ratio is expected to be lower than during this laboratory study. Thus, surface saturation will exert an important influence on reaction rates in nature.

© 2003 Elsevier B.V. All rights reserved.

**Keywords:** Ferrihydrite; Hydrogen sulfide; Kinetics; Iron oxide; Dissolution; Oxidation

## 1. Introduction

Iron is one of the few major elements to undergo extensive redox cycling in surface and near-surface environments. The iron present in the form of (oxyhydr)oxides represents an important component of rocks and soils, and accounts for approximately 2.1 wt.% of the oxidized sediments transported to lacus-

\* Present address: Danish Center for Earth System Science, Institute of Biology, University of Southern Denmark, Campusvej 55, DK-5230 Odense, Denmark. Tel.: +45-65-502745.

E-mail address: s.poulton@biology.sdu.dk (S.W. Poulton).

trine and marine environments on a global scale (Poulton and Raiswell, 2002). Iron oxides are efficient scavengers of trace metals, organics and ligands such as phosphate (e.g. Tipping, 1981; Salomons and Forstner, 1984; Poulton and Raiswell, 2000), which may be extensively released to solution during reductive dissolution. Hydrogen sulfide is an important reductant of iron oxides, and may be the major pathway for the reductive dissolution of iron oxides in sulfidic sediments and euxinic basins (Canfield, 1989; Kostka and Luther, 1995; Krom et al., 2002).

Several studies have used different approaches to evaluate the kinetics and mechanism of the reaction between iron (oxyhydr)oxides and dissolved sulfide. Rickard (1974) and Pyzik and Sommer (1981) examined the rates of formation of iron monosulfide during the sulfidation of goethite. Dos Santos Afonso and Stumm (1992) applied a surface speciation model to investigate the reductive dissolution of hematite by hydrogen sulfide, under conditions of undersaturation with respect to iron monosulfide. Peiffer et al. (1992) examined the specific oxidation of H<sub>2</sub>S by lepidocrocite, while Yao and Millero (1996) investigated the oxidation of dissolved sulfide by freshly precipitated hydrous ferric oxide. Canfield and Berner (1987) estimated the in situ reduction rate of magnetite by dissolved sulfide in an anoxic marine sediment. Recently, Poulton et al. (2002, 2003) examined the kinetics of dissolved sulfide removal by ferrihydrite under flow-through conditions. The aforementioned studies all highlight the importance of oxide surface area, dissolved sulfide concentration and pH to reaction rates. However, the specific impact of dissolved sulfide concentration on reaction rates is unclear. Previous studies of the oxidation of dissolved sulfide by iron (oxyhydr)oxides (Peiffer et al., 1992; Yao and Millero, 1996) imply a first order relationship between the initial sulfide concentration and sulfide oxidation rates. Dos Santos Afonso and Stumm (1992) similarly determined a first order reaction with respect to the concentration of surface-complexed sulfide during the reductive dissolution of hematite. By contrast, Pyzik and Sommer (1981) and Canfield and Berner (1987) suggest a fractional order relationship (0.5) between dissolved sulfide and reductive dissolution rates. Furthermore, Rickard (1974) reported a reaction order of 1.5 for total dissolved sulfide during the formation of FeS from goethite. It is important to resolve these

differing observations to enable a realistic assessment of the reactivity of different iron (oxyhydr)oxide minerals towards dissolved sulfide in natural sulfidic environments (e.g. Canfield et al., 1992).

The adsorption of dissolved species at the oxide surface may greatly affect the ligand-promoted reductive dissolution of iron (oxyhydr)oxides (Bondietti et al., 1993; Biber et al., 1994; Yao and Millero, 1996). Yao and Millero (1996) examined the effects of pre-adsorption of various seawater solutes to freshly precipitated hydrous ferric oxide and found that phosphate, silicate, sulfate, magnesium and calcium significantly decreased sulfide oxidation rates. Biber et al. (1994) investigated the impact of various inorganic and organic ligands on the reductive dissolution of goethite and hematite by H<sub>2</sub>S in 0.1 M NaClO<sub>4</sub>, and employed a surface complexation model to estimate the extent of inhibition due to phosphate and sulfate as a function of pH. However, no studies have directly measured the effect of competitive adsorption of seawater solutes as a function of pH. Competitive adsorption may exert a significant impact on reaction rates following the initial dissolution of the oxide surface (Poulton et al., 2003).

In the present study, current understanding of the reaction mechanism between dissolved sulfide and iron (oxyhydr)oxides is applied to experimental data for two-line ferrihydrite, with three main aims:

- (I) To evaluate the kinetics for the reaction of dissolved sulfide with two-line ferrihydrite in seawater and to present the first combined dataset on rates of both sulfide oxidation and Fe(II) dissolution.
- (II) To explain the differing reaction orders obtained by previous studies with respect to the rate dependency of dissolved sulfide concentration.
- (III) To determine the impact of competitive adsorption of major seawater solutes on reaction rates.

## 2. Methods

### 2.1. Materials

All chemicals were Analytical Reagent grade and all solutions were prepared in MilliQ water. Synthetic two-line ferrihydrite was prepared by titration of a 50 mM

solution of  $\text{Fe}(\text{NO}_3)_3 \cdot 9\text{H}_2\text{O}$  to pH 6.5 with 1 M KOH (Schwertmann and Cornell, 1991). After hydrolysis, the ferrihydrite was washed thoroughly to remove traces of nitrate and then freeze-dried. The ferrihydrite was characterised using a Phillips PW1050 XRD with Cu  $K\alpha$  radiation. Surface area was determined by the multi-point BET method (using a Beckman/Coulter SA 1300 analyser with a Beckman/Coulter SA-PREP out-gasser) as  $299 \text{ m}^2 \text{ g}^{-1}$ .

Stock sulfide solutions were prepared by dissolving rinsed  $\text{Na}_2\text{S} \cdot 9\text{H}_2\text{O}$  crystals in  $\text{N}_2$ -purged water. The  $\text{N}_2$  (99.999%) used in this study was further purified by passing through an Alltech oxygen trap and then an Alltech indicating oxygen trap. Artificial seawater was prepared according to the recipe of Millero (1986).

## 2.2. Experimental

The experimental apparatus consisted of a 1 l air-tight glass vessel, into which a pH electrode and ports for sample removal, degassing and deoxygenated HCl addition were inserted by gas-tight screw plugs. Experiments were performed in constantly stirred (using a glass-coated magnetic stirrer) artificial seawater or 0.42 M NaCl over the pH range 4.0–8.2. The initial dissolved sulfide concentration range was 150–1200  $\mu\text{M}$  and the initial ferrihydrite surface area varied between 10 and 120  $\text{m}^2 \text{ l}^{-1}$  (Table 1). The temperature was maintained at 25 °C with a Techne water bath and light was excluded from all experiments. An appropriate volume of stock sulfide solution was added to the deoxygenated (by degassing for 1 h) aqueous medium via an air-tight syringe. The solution was then adjusted to the required pH by the addition of deoxygenated 0.1 M HCl and the initial dissolved sulfide concentration was measured in triplicate. A known weight of ferrihydrite was degassed for 1 h in 10 ml of MilliQ water in an air-tight glass chamber attached directly to the closed sampling port of the reaction vessel. The slurry was then added to the vessel by changing the  $\text{N}_2$  flow direction and opening the input valve. This process took approximately 2–5 s (note that the other ports on the vessel remained closed during this process and thus no  $\text{H}_2\text{S}_g$  was flushed from the system) and then the input port was immediately closed. This ensured

Table 1

Initial conditions for each experiment (AS=artificial seawater; NaCl=0.42 M, sulfate=28.9 mM)

Run no.	pH	Ferrihydrite surface area ( $\text{m}^2 \text{ l}^{-1}$ )	Initial $\Sigma\text{S}^{2-}$ ( $\mu\text{M}$ )	Aqueous medium
1	7.5	100	1136	AS
3	7.5	100	1046	AS
4	7.5	100	520	AS
5	7.5	100	248	AS
6	7.5	50	521	AS
7	7.5	75	543	AS
8	7.5	100	543	AS
9	7.5	100	519	NaCl
10	6.5	100	517	AS
11	6.0	100	508	AS
14	4.5	100	537	AS
15	4.0	100	512	NaCl
16	8.2	100	553	NaCl
17	8.2	100	548	AS
18	4.0	100	502	AS
19	5.45	100	511	AS
20	7.5	10	560	AS
21	7.5	100	528	NaCl + $\text{SO}_4^{2-}$
22	6.0	100	504	NaCl + $\text{SO}_4^{2-}$
23	4.0	100	504	NaCl + $\text{SO}_4^{2-}$
24	7.0	100	544	NaCl + $\text{SO}_4^{2-}$
30	8.2	100	537	NaCl + $\text{SO}_4^{2-}$
39	7.5	100	513	AS
41	5.45	100	465	NaCl
42	7.0	100	536	NaCl
43	6.0	100	511	NaCl
44	7.5	100	403	AS
48	7.5	80	560	AS
49	7.5	120	573	AS
50	7.5	100	844	AS
51	7.5	100	196	AS
53	5.0	100	554	NaCl
54	5.0	100	547	NaCl + $\text{SO}_4^{2-}$
66	7.5	100	192	AS

that the ferrihydrite slurry remained completely anoxic during addition to the reaction vessel. An additional experiment was performed in which the ferrihydrite slurry was degassed for 18 h prior to addition to the reaction vessel. The longer degassing time resulted in no detectable change in the measured reaction rates or products. The reaction with sulfide consumes protons and thus the pH was controlled via a pH-stat by the addition of deoxygenated 0.1 M HCl. By using this system, interferences with pH buffers were avoided. Samples were periodically removed from the reaction vessel with

a syringe for immediate analysis. To ensure experiments were performed under constant anaerobic conditions a blank run (containing approximately 1000  $\mu\text{M}$  dissolved sulfide) with no ferrihydrite was made. No detectable decrease in dissolved sulfide was observed over an 18 h period (all experiments were completed within 2 h).

The solubility constant ( $K_s$ ) of amorphous  $\text{FeS}_s$  for the reaction  $\text{FeS}_s + \text{H}^+ = \text{Fe}^{2+} + \text{HS}^-$  has a value given by  $K_s = 10^{-3.03 \pm 0.12}$  (Davison et al., 1999). Activity coefficients for a salinity of 35‰ were taken from Davison (1980). Under the experimental conditions of the present study, an average ion activity product (IAP) of  $10^{-2.51}$  was obtained at pH 7.5, indicating saturation with respect to amorphous  $\text{FeS}_{(s)}$ .

### 2.3. Analytical

Dissolved Fe(II) and Fe(III) were measured on 1-ml samples by the revised ferrozine method of Viollier et al. (2000). Dissolved Fe(III) was below detection ( $<0.5 \mu\text{M}$ ) in all experiments. Replicate determinations of a stock Fe(II) solution gave a mean of  $7.1 \pm 0.3 \mu\text{M}$  ( $2\sigma$ ,  $n=6$ ). The formation of aqueous FeS has been observed in both laboratory (e.g. Zhang and Millero, 1994; Luther et al., 1996; Theberge and Luther, 1997; Davison et al., 1999) and field studies (e.g. Rickard et al., 1999; Luther et al., 2001).  $\text{FeS}_{\text{aq}}$  may contribute significantly to the total dissolved Fe pool at  $\text{pH} \geq 7$  (Luther et al., 1996; Zhang and Millero, 1994). Luther et al. (1996) report that soluble FeS complexes dissociate below pH 7, releasing  $\text{H}_2\text{S}$  from solution. Thus,  $\text{FeS}_{\text{(aq)}}$  was measured as part of the dissolved Fe(II) pool after addition of the acidic ferrozine reagent. Total solid phase Fe(II) was determined after the addition of 0.5 ml of unfiltered sample to 0.5 ml of 1 N HCl. The sample was immediately purged with  $\text{N}_2$  to dispel  $\text{H}_2\text{S}$ . Samples for Fe(II) were analysed after 30 min using the ferrozine assay (Stookey, 1970). The Fe(II) concentration in the resulting 0.5 N HCl extraction remained constant over a period of at least 1 h (see also Lovely and Phillips, 1987; Fredrickson et al., 1998) indicating that the method does not result in the oxidation of Fe(II) or the reduction of Fe(III). The 0.5 N HCl extraction was tested relative to a 6 N HCl extraction, which dissolved the solid phase entirely. The 0.5 N HCl treatment quantitatively extracted all

solid phase Fe(II). The Fe(II) sorbed to particles was measured using the ferrozine assay following extraction in buffered (pH 7) 1 M  $\text{CaCl}_2$  for 2 h (Heron et al., 1994). After addition of the  $\text{CaCl}_2$ , the samples were immediately purged with  $\text{N}_2$  to dispel  $\text{H}_2\text{S}$ . Previous studies have demonstrated that sorbed Fe(II) is quantitatively extracted by this method and is stable over the time period of the extraction (Heron et al., 1994).

Dissolved and solid phase sulfur (with the exception of dissolved sulfate) was analysed by standard spectrophotometric techniques. Potential interferences between different sulfur species when using these techniques have previously been investigated (e.g. Chen and Morris, 1972; O'Brien and Birkner, 1977; Pyzik and Sommer, 1981) and where appropriate samples were treated prior to analysis. Dissolved sulfide was measured on filtered (0.2  $\mu\text{m}$ ) samples by the methylene blue method (Cline, 1969). Replicate measurements of a stock sulfide solution gave a mean of  $1088 \pm 12 \mu\text{M}$  ( $2\sigma$ ,  $n=8$ ). Freshly formed  $\text{FeS}_s$  is dissolved by the 6 N HCl present in the diamine reagent, and thus this method was also used to measure total sulfide (i.e. dissolved plus solid) in unfiltered samples. Filtered (0.2  $\mu\text{m}$ ) samples (1 ml) were periodically analysed for thiosulfate, sulfite, polysulfides and sulfate. Immediately after collection, these samples were injected through a septum into 1.5 ml glass vials, which had previously been flushed with  $\text{N}_2$ . Sulfite was measured after stabilising with sodium tetrachloromercurate, as the *p*-rosaniline hydrochloride complex in formaldehyde solution (West and Gaeke, 1956). Thiosulfate and sulfate samples were initially added to 0.1 ml of 0.5 M  $\text{ZnCl}_2$  to precipitate dissolved sulfide. Thiosulfate was determined immediately after filtration (to remove ZnS) by the copper catalysed acid cyanolysis of thiosulfate to thiocyanate (Urban, 1961). Sulfate was measured in experiments performed in 0.42 M NaCl using a Dionex DX-100 Ion Chromatograph. Polysulfide sulfur was measured following conversion to thiosulfate, by a modification of the technique described by Luther (1985); the filtered sample was added to a  $\text{N}_2$ -flushed vial containing 0.1 ml of 0.1 M  $\text{Na}_2\text{SO}_3$  and heated for 2 h at 60 °C. The dissolved sulfide was then fixed in 0.1 ml of 0.5 M  $\text{ZnCl}_2$  and the sample was filtered (0.2  $\mu\text{m}$ ) and analysed for thiosulfate as described above. Polysulfide sulfur was then estimated after subtraction of the original thiosulfate

concentration. This method has not been extensively tested and thus the polysulfide measurements are considered to be semi-quantitative. Elemental sulfur was determined on unfiltered samples as the  $\text{FeSCN}^+$  complex after cyanolysis in acetone (Bartlett and Skoog, 1954). Total oxidised sulfur was determined as the difference between the initial sulfide concentration and the total sulfide concentration (solid plus dissolved) measured at a particular time interval (see also Yao and Millero, 1996).

#### 2.4. Surface complexation modeling

Surface complexation modeling was performed using the diffuse double layer model, for which equilibrium constants have been defined for the specific adsorption of various chemical species to hydrous ferric oxide (Dzombak and Morel, 1990). The model considers surface sites and complexes to lie in a layer on the mineral surface, with a net electrical charge which is balanced by an outer diffuse layer. The model was implemented using the computer program PHREEQC (Parkhurst and Appelo, 1999). Model surface complexation constants considered in this study are listed in Table 2. The adsorption constants for  $>\text{FeS}^-$  and  $>\text{FeSH}$  were taken from Peiffer et al. (1992) and were originally determined

for sulfide complex formation at the hematite surface (Dos Santos Afonso and Stumm, 1992). These constants have previously been used to investigate sulfide complexation on goethite (Biber et al., 1994) and lepidocrocite surfaces (Peiffer et al., 1992). Mather (1995) produced a sorption database for goethite, and found similar surface complexation constants for the sorption of ions to goethite and hydrous ferric oxide. This implies that the reaction energy at the individual surface hydroxyl group is essentially the same for different iron (oxyhydr)oxides. Thus, it is appropriate to apply the hematite sulfide complexation constants to hydrous ferric oxides. Nevertheless, errors in the model calculations are a direct reflection of uncertainties regarding these equilibrium constants, in addition to uncertainties regarding the total surface concentration of metal centres (site density), and the fact that the theory does not account for the kinetics of sorption reactions.

### 3. Results

#### 3.1. Iron and sulfur speciation

The removal of dissolved sulfide and the formation of iron and sulfur species during the reaction with two-line ferrihydrite are shown for a representative experiment in Fig. 1. The majority of the dissolved sulfide was rapidly oxidised (Fig. 1a). Samples were periodically analysed for oxidised sulfur species, and elemental sulfur was found to be the dominant oxidation product, with lesser concentrations of polysulfide sulfur (5–10% at pH 7.5). No higher oxidation state sulfur species were detected. These findings are consistent with previous studies of sulfide oxidation by hydrous ferric oxide (Yao and Millero, 1996). The formation of solid phase FeS accounted for only 15–30% of the total initial sulfide concentration in experiments performed at pH 7.5, with relatively higher proportions formed at higher initial sulfide concentrations and lower ferrihydrite surface areas.

The majority of the Fe(II) produced at pH 7.5 remained associated with the oxide surface on the time-scale of these experiments (Fig. 1b). However, sorbed Fe(II) (i.e. that which has been adsorbed at the oxide surface after a dissolution step) was a

Table 2  
Equilibrium constants used in the present study

Surface species	log $K$
$>\text{FeOH}$	0.0
$>\text{FeOH}_2^+$	7.29
$>\text{FeO}^-$	-8.93
$>\text{FeSH}$	10.82 <sup>a</sup>
$>\text{FeS}^-$	5.3 <sup>a</sup>
$>\text{FeS}^-$ (deprotonation of $>\text{FeSH}$ )	-5.5 <sup>b</sup>
$>\text{FeONa}$	-8.6
$>\text{FeOH}_2\text{Cl}$	7.5
$>\text{FeOHSO}_4^-$	0.79
$>\text{FeSO}_4^{2-}$	7.78
$>\text{FeOCa}^+$	-5.85
$>\text{FeOHCa}^{2+}$	4.97
$>\text{FeOMg}^+$	-4.6

Surface complexation constants from Dzombak and Morel (1990) except <sup>a</sup>Peiffer et al. (1992) and <sup>b</sup>Dos Santos Afonso and Stumm (1992). The dissociation constant used in model calculations for  $\text{H}_2\text{S}$  in seawater (log  $K_1^* = 6.524$ ) was taken from Millero et al. (1988).

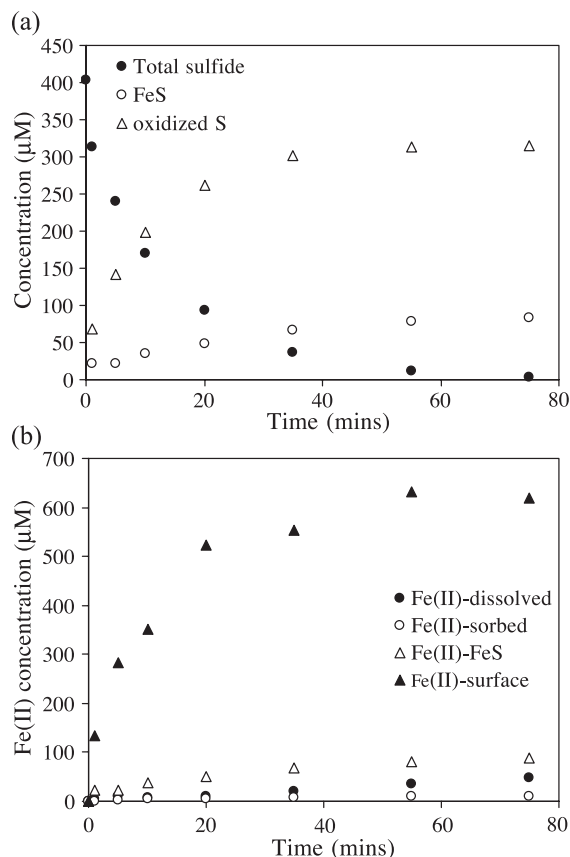


Fig. 1. Speciation of sulfur (a) and iron (b) for an experiment with two-line ferrihydrite (surface area =  $100 \text{ m}^2 \text{ l}^{-1}$ ) in seawater at pH 7.5.

minor component, accounting for <2% of the total Fe(II) produced in all experiments. Supporting evidence for the fact that the majority of the surface-associated Fe(II) does not occur from re-adsorption following dissolution, comes from experiments performed at lower pH. Fig. 2 shows data produced during an experiment at pH 5.45. Under these conditions, FeS occurs only as a transient phase, and the surface Fe(II) initially increases followed by a decrease as Fe(II) continues to be released to solution (at a faster rate than that seen at higher pH; Fig. 1). Iron(II) does not extensively adsorb to Fe (oxyhydr)oxides at this pH (e.g. Zhang et al., 1992) and was below detection. Fig. 2 clearly shows that the surface Fe(II) continues to detach from the oxide surface for a considerable period of

time after all the sulfide has reacted from solution. Thus, the dissolution of Fe(II) is a slow process relative to the overall reduction of Fe(II) by sulfide, and this (and not re-adsorption of dissolved Fe) accounts for the high concentrations of surface-bound Fe(II) found at pH 7.5 (Fig. 1).

The reduced iron present as amorphous iron monosulfide was determined from the analysis of solid phase sulfide, assuming a composition  $\text{Fe}_{1.05}\text{S}$  (Berner, 1964; note that small variations in the assumed composition of FeS have little effect on calculated reaction kinetics). This phase accounted for 7–15% of the total Fe(II) produced at pH 7.5 (Fig. 1). The total concentration of Fe(II) was approximately double the concentration of sulfur oxidised at each time interval, consistent with the two electron transfer required to oxidise dissolved sulfide to elemental S or zero valent polysulfide S. Dissolved Fe(II) accounted for <10% of the total Fe(II) produced at pH 7.5, but was progressively more important at lower pH.

### 3.2. Rates of Fe dissolution and $\text{H}_2\text{S}$ oxidation

Fig. 3 shows representative data for the total dissolution of ferrous iron. It should be noted that, in the environment, it is the Fe(II) dissolution rate and not the Fe reduction rate that controls the rate of Fe (oxyhydr)oxide sulfidation (the Fe reduction rate simply approximates to double the sulfide

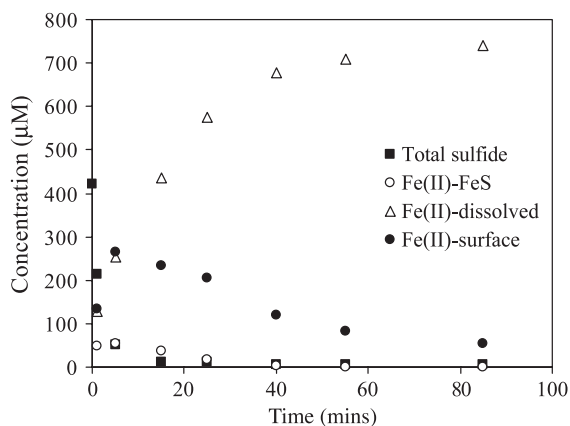


Fig. 2. Total sulfide and Fe phases during an experiment with two-line ferrihydrite (surface area =  $100 \text{ m}^2 \text{ l}^{-1}$ ) in 0.42 M NaCl at pH 5.45.

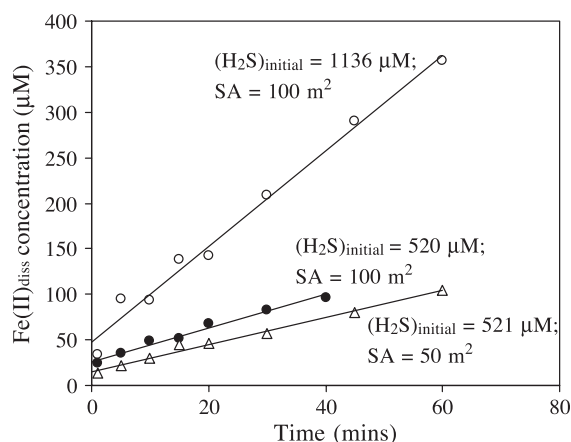


Fig. 3. Representative data for the reductive dissolution of two-line ferrihydrite at pH 7.5 in seawater.

oxidation rate). Hence, this study concentrates on the rate of Fe(II) dissolution. The total concentration of dissolved Fe(II) produced was calculated as the sum of dissolved, sorbed and monosulfide iron. The linear relationship evident in Fig. 3 implies that the dissolution reaction follows a heterogeneous zero-order rate law with respect to dissolved Fe(II). A similar observation was made for the dissolution of hematite by  $H_2S$  (Dos Santos Afonso and Stumm, 1992).

The dissolution of ferrihydrite at a given pH can be expressed by an empirical rate equation of the form:

$$\frac{d(Fe^{2+})_{diss}}{dt} = k_{Fe}(H_2S)_{t=0}^a A^b \quad (1)$$

where  $(Fe^{2+})_{diss}$  is the total dissolved  $Fe^{2+}$  concentration,  $(H_2S)_{t=0}$  is the initial total sulfide concentration,  $A$  is the initial ferrihydrite surface area,  $a$  and  $b$  are the reaction orders with respect to  $(H_2S)_{t=0}$  and  $A$ , respectively, and  $k_{Fe}$  is the overall rate constant. A similar rate expression may be written for the oxidation of dissolved sulfide,  $(H_2S)_{tot}$ :

$$-\frac{d(H_2S)_{tot}}{dt} = k_s(H_2S)_{t=0}^a A^b \quad (2)$$

Various methods may be used to determine the reaction orders,  $a$  and  $b$ . When the surface area is in excess, the reaction order with respect to

$(H_2S)_{t=0}$  for the oxidation of sulfide (Eq. (2)) may be determined by fitting the data to various rate equations with different values for the reaction order,  $a$ . Plots of  $\ln(H_2S)_{tot}$  vs. time decrease linearly for the reaction with ferrihydrite (Fig. 4), suggesting a pseudo-first order rate constant for the dependency of sulfide oxidation rate on sulfide concentration for each individual experiment. The rapid decrease in sulfide concentration during the first minute of the reaction (Fig. 4) is likely due to a pre-equilibrium phase with respect to the adsorption of sulfide at the oxide surface (see Dos Santos Afonso and Stumm, 1992).

Although the data presented in Fig. 4 suggest a first order dependency of sulfide oxidation rate on  $(H_2S)_{tot}$  for each individual experiment, the slopes of the lines imply that reaction rates are relatively increased at lower initial sulfide concentrations. This observation is further highlighted when initial rate theory is used to determine the reaction order,  $a$ , for rates of both sulfide oxidation and Fe(II) dissolution. Initial rate theory relates the initial concentrations of reactants to the initial reaction rate. In the present study, it is the rates of sulfide oxidation and Fe dissolution, which are of interest. A study incorporating the kinetics for the initial rapid pre-equilibrium sulfide adsorption step would require more sophisticated monitoring techniques than those employed here. Thus, the initial reaction rate was determined in relation to the data obtained after the start of the

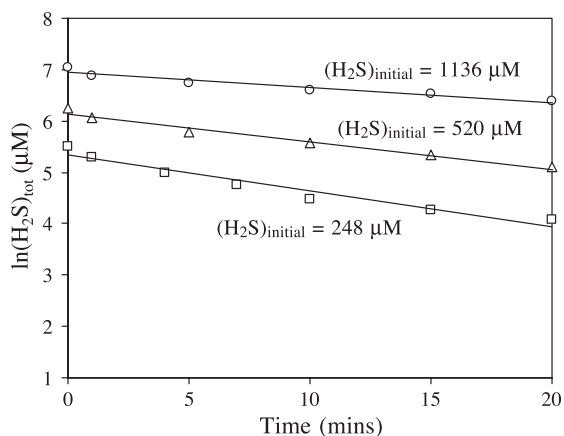


Fig. 4. Plot of  $\ln(H_2S)_{tot}$  vs. time for the oxidation of  $H_2S$  by two-line ferrihydrite ( $100 \text{ m}^2 \text{ l}^{-1}$ ) in seawater (pH=7.5).

experiment (i.e. the concentrations of dissolved sulfide and iron at  $t=0$  are not included in this data treatment). Iron(II) dissolution rates were linear with time (Fig. 3) and thus rates were determined by regression analysis over the entire extent of the monitored reaction. Rates of sulfide oxidation decrease significantly as sulfide is removed from solution (Fig. 1). Thus, the initial reaction rate was determined by regression analysis of the initial linear phase of sulfide removal. All regression equations were applied over the region where the error on the slope was within 5%. The  $y$ -axis intercept of these regression lines gives an estimate of the sulfide available for reaction after the initial adsorption step (i.e. the measured initial sulfide concentration minus the estimate obtained by linear regression approximates the concentration of surface-complexed sulfide), and these estimates were used as the initial dissolved sulfide concentration.

The slopes of the lines in Fig. 5 imply that, when experiments performed over the entire dissolved sulfide range (150–1200  $\mu\text{M}$ ) are considered, a square root order may be more appropriate to describe the dependency of the reaction on initial sulfide concentration. The reaction order with respect to surface area was determined experimentally by varying the initial ferrihydrite surface area at constant pH (7.5) and initial dissolved sulfide concentration (500  $\mu\text{M}$ ). The resulting slopes (Fig. 6)

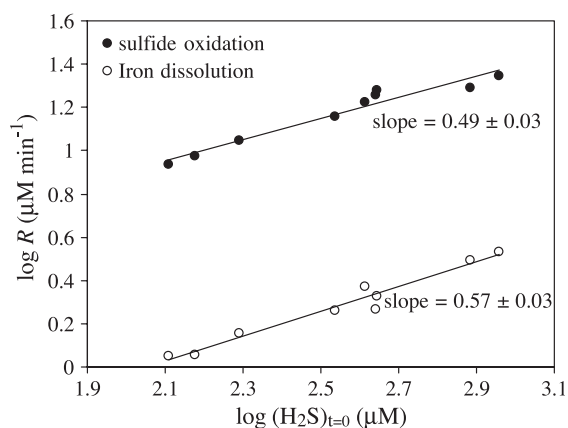


Fig. 5. Plot of log reaction rate ( $R$ ) vs. log initial sulfide concentration ( $(\text{H}_2\text{S})_{t=0}$ ) for experiments with two-line ferrihydrite ( $100 \text{ m}^2 \text{ l}^{-1}$ ) at pH 7.5 in seawater.

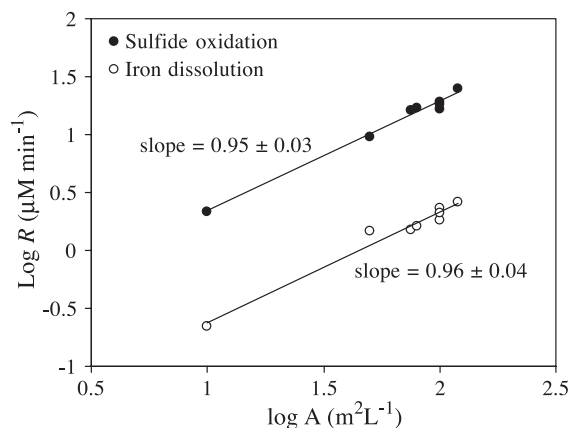


Fig. 6. Plot of log reaction rate ( $R$ ) vs. log initial surface area ( $A$ ) for experiments with two-line ferrihydrite at pH 7.5 in seawater ( $(\text{H}_2\text{S})_{t=0} = 500 \mu\text{M}$ ).

of  $0.95 \pm 0.03$  for sulfide oxidation and  $0.96 \pm 0.04$  for Fe(II) dissolution indicate a first order reaction with respect to surface area. Determination of the reaction orders with respect to surface area and initial sulfide concentration gives the following rate expression:

$$R_i = k_i (\text{H}_2\text{S})_{t=0}^{0.5} A \quad (3)$$

where  $R_i$  represents the rate of sulfide oxidation ( $-\text{d}(\text{H}_2\text{S})_{\text{tot}}/\text{d}t$ ;  $R_S$ ) or Fe(II) dissolution ( $\text{d}(\text{Fe}^{2+})_{\text{diss}}/\text{d}t$ ;  $R_{\text{Fe}}$ ) and  $k_i$  represents the appropriate rate constant ( $k_S$  or  $k_{\text{Fe}}$ ). The apparent rate constants were determined as  $k_S = 8.4 \times 10^{-6} \pm 0.9 \times 10^{-6} \text{ mol}^{0.5} \text{ l}^{0.5} \text{ m}^{-2} \text{ min}^{-1}$  and  $k_{\text{Fe}} = 1.1 \times 10^{-6} \pm 0.2 \times 10^{-6} \text{ mol}^{0.5} \text{ l}^{0.5} \text{ m}^{-2} \text{ min}^{-1}$  ( $n=14$ ) when  $R_i$  is expressed in  $\text{mol l}^{-1} \text{ min}^{-1}$ ,  $(\text{H}_2\text{S})_{t=0}$  is expressed in  $\text{mol l}^{-1}$  and  $A$  is expressed in  $\text{m}^2 \text{ l}^{-1}$ .

### 3.3. Effect of pH on reaction kinetics

Fig. 7 shows the effect of pH on the reaction constants,  $k_S$  and  $k_{\text{Fe}}$ , for two-line ferrihydrite in seawater and in 0.42 M NaCl. Reaction rates are considerably slower at lower pH in seawater relative to 0.42 M NaCl, while rates are comparable above  $\sim \text{pH } 7.5$ . Maximum rates of sulfide oxidation occur near a pH of 6 for seawater, which shifts to  $\sim 5.5$  for 0.42 M NaCl. The maximum corresponding rates for



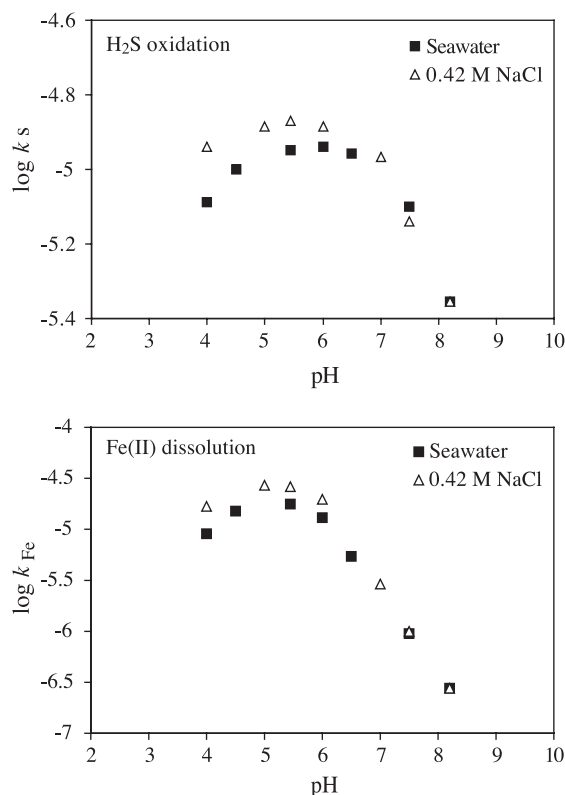


Fig. 7. Effect of pH on rate constants  $k_S$  and  $k_{Fe}$  for seawater and 0.42 M NaCl ( $100 \text{ m}^2 \text{ l}^{-1}$  two-line ferrihydrite;  $(\text{H}_2\text{S})_{t=0} = 500 \text{ } \mu\text{M}$ ).

the dissolution of iron occur at slightly more acidic conditions (near pH 5.5 and 5 for seawater and 0.42 M NaCl, respectively).

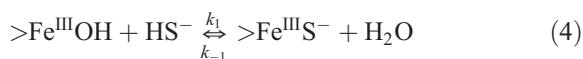
## 4. Discussion

### 4.1. Reaction mechanism

The experimental determination of first order reaction kinetics with regard to ferrihydrite surface area (Fig. 5) implies a surface-controlled process, and is consistent with previous studies (Pyzik and Sommer, 1981; Dos Santos Afonso and Stumm, 1992; Peiffer et al., 1992; Yao and Millero, 1996). The reaction between iron oxides and dissolved sulfide has been suggested to proceed via the fol-

lowing reaction sequence (Dos Santos Afonso and Stumm, 1992):

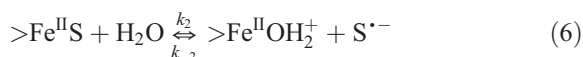
(I) Surface complex formation:



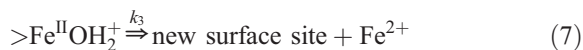
(II) Electron transfer:



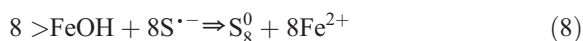
(III) Release of the oxidized product:



(IV) Detachment of Fe(II):



Surface complex formation (Eq. (4)) is generally assumed to occur rapidly at the oxide surface, followed by electron transfer (Eq. (5)). The  $\text{HS}^-$  and surface  $\text{Fe}^{3+}$  are able to form an inner sphere complex (adsorbate is directly coordinated by the surface), which is expected to result in the faster transfer of electrons than an outer sphere process alone (Luther, 1990). The  $\text{S}^{\cdot-}$  radical is then released (Eq. (6)) and rapidly reduces additional Fe(III) ions, to form higher oxidation state sulfur species. The Fe(II) produced at the oxide surface is then released to solution (Eq. (7)). In the case of sulfide oxidation by ferrihydrite, the final oxidised sulfur product is elemental sulfur (Eq. (8)), and the Fe(II) released may react with additional dissolved sulfide to produce  $\text{FeS}_s$  (Eq. (9)):



The apparent rate constants for the oxidation of sulfide ( $k_S = 8.4 \times 10^{-6} \pm 0.9 \times 10^{-6} \text{ mol}^{0.5} \text{ l}^{0.5} \text{ m}^{-2} \text{ min}^{-1}$ ) and the dissolution of Fe(II) ( $k_{Fe} = 1.1 \times 10^{-6} \pm 0.2 \times 10^{-6} \text{ mol}^{0.5} \text{ l}^{0.5} \text{ m}^{-2} \text{ min}^{-1}$ ) indicate that the dissolution of Fe(II) is approximately 15 times slower than the oxidation of sulfide (given that the ratio

of sulfide oxidised to Fe(II) produced is 2:1). This implies that the detachment of Fe(II) from the oxide surface is the overall rate limiting step (see also Pyzik and Sommer, 1981; Zinder et al., 1986; Hering and Stumm, 1990; Stumm and Wieland, 1990). However, the proposed reaction mechanism suggests that dissolution of surface Fe(II) is required prior to further oxidation of dissolved sulfide. This is not inconsistent with slower rates of Fe(II) dissolution relative to sulfide oxidation as determined in this study, because different surface sites and different forms of surface-complexed sulfide react at different rates (see Yao and Millero, 1996 and later discussion). Therefore the most reactive sites rapidly oxidize sulfide, and the rate at which the Fe(II) produced at these sites is detached from the surface depends on the extent of protonation of the nearest attached oxide or hydroxide ion (Zinder et al., 1986). After dissolution, new surface sites are available to complex dissolved sulfide (Eq. (7)). By contrast, less reactive sites and less reactive complexed-sulfide species release oxidized S and Fe(II) at a slower rate, and thus generate new surface sites at a slower rate. Thus, sulfide can initially continue to be oxidized without the generation of new surface sites.

The determination of a fractional order dependency on sulfide concentration is in agreement with previous studies of the reductive dissolution of iron (oxyhydr)oxides (Pyzik and Sommer, 1981; Canfield and Berner, 1987). However, previous studies of the oxidation of sulfide suggest a first order reaction with respect to the initial dissolved sulfide concentration (Peiffer et al., 1992; Yao and Millero, 1996), while Dos Santos Afonso and Stumm (1992) similarly determined a first order dependency for surface-complexed sulfide during the reductive dissolution of hematite. Rickard (1974) determined a reaction order of 1.5 for total dissolved sulfide during the formation of FeS<sub>s</sub>. However, Rickard (1974) monitored the rate of change of hydrogen ion activity and related that concentration via stoichiometric relations to the rate of FeS formation. Thus, the rate expression modeled the entire reaction (adsorption, reduction, dissolution and precipitation of FeS<sub>s</sub>) and is therefore not comparable to subsequent studies. The following discussion attempts to reconcile the remaining contrasting observations outlined above.

Fig. 8 demonstrates that the relative increase in rates of sulfide oxidation and Fe(II) dissolution pro-

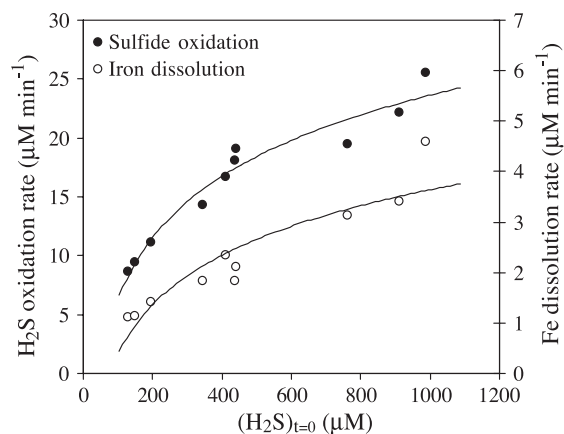


Fig. 8. Rates of sulfide oxidation and Fe(II) dissolution as a function of  $(\text{H}_2\text{S})_{t=0}$  ( $100 \text{ m}^2 \text{ l}^{-1}$  two-line ferrihydrite; pH = 7.5).

gressively lessens as the initial sulfide concentration increases. Previous studies of the reductive dissolution of iron (oxyhydr)oxides by reductants other than sulfide suggest that such a trend may be indicative of surface saturation with respect to the reductant at higher initial dissolved concentrations (see Banwart et al., 1989; Dos Santos Afonso et al., 1990; Suter et al., 1991). Surface complexation modeling provides supporting evidence for surface saturation at higher initial dissolved sulfide concentrations. Dos Santos Afonso and Stumm (1992) evaluated the dissolution of hematite in terms of the following expression (considering surface complex formation as a rapid pre-equilibrium step):

$$\frac{d[\text{Fe(II)}]}{dt} = \frac{2k_2k_3k_{\text{et}}}{k_2k_3 + k_{-\text{et}}(k_3 + k_{-2}[\text{S}^{\bullet-}])} \{>\text{FeS}^-\} \quad (10)$$

where the components of this expression relate to Eqs. (4)–(7), and  $\{>\text{FeS}^-\}$  is the concentration of surface complex. A similar expression may be derived for the oxidation of dissolved sulfide:

$$-\frac{d[\text{HS}^-]}{dt} = \frac{2k_2k_3k_{\text{et}}}{k_2k_3 + k_{-\text{et}}(k_3 + k_{-2}[\text{S}^{\bullet-}])} \{>\text{FeS}^-\} \quad (11)$$

Eqs. (10) and (11) give the Fe(II) dissolution rate ( $R_{\text{Fe}}$ ) or the sulfide oxidation rate ( $R_{\text{S}}$ ) in terms of the

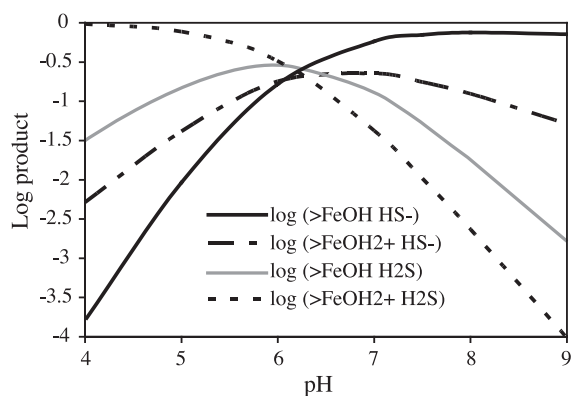
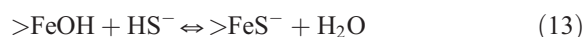


Fig. 9. The mole fractions of reactants in Eqs. (13)–(16) as a function of pH (see text for details).

surface concentration of  $>FeS^-$ , assuming a steady state concentration for the intermediate product  $S^{*-}$ :

$$R_i = k_a \{>FeS^-\} \quad (12)$$

Eqs. (4)–(6) and Eqs. (10)–(12) are written in terms of the  $HS^-$  aqueous species and the surface species  $>FeS^-$ . Yao and Millero (1996) evaluated the importance of a range of sulfide surface species during the reaction with hydrous ferric oxide and found that reaction rates could best be explained by a combination of the following reaction pathways over the pH range 3–9:



The availability of reactants for Eqs. (13)–(16) is highly pH-dependent. The speciation of dissolved sulfide can be represented by:

$$\alpha_{H_2S} = [H_2S]/[H_2S]_{tot} \quad (17)$$

$$\alpha_{HS^-} = [HS^-]/[H_2S]_{tot} \quad (18)$$

and was calculated using the dissociation constant for  $H_2S$  at 25 °C in seawater ( $\log K_1^* = 6.524$ ; Millero et al., 1988). The surface speciation of ferrihydrite is given by:

$$\alpha_{>FeOH} = [>FeOH]/S_T \quad (19)$$

$$\alpha_{>FeOH_2^+} = [>FeOH_2^+]/S_T \quad (20)$$

where  $S_T$  represents the total concentration of surface sites. The mole fractions of  $>FeOH$ ,  $>FeOH_2^+$  and in addition to  $S_T$ , were calculated using the surface complexation model. Fig. 9 shows the product of the reactant fractions as a function of pH. At pH 7.5, the availability of reactants for reaction 16 is relatively reduced compared to reactions 13–15 (only 1% of the total), implying that the surface species  $>FeS^-$  and  $>FeHS$  are likely to dominate. Thus, in the following discussion, only the surface species  $>FeS^-$  and  $>FeHS$  are considered.

Surface complex formation equilibria have previously been estimated for  $>FeS^-$  and  $>FeHS$  (Table 2). Fig. 10 shows model results for the surface concentrations of sulfide species as a function of total dissolved sulfide, based on these surface complex formation constants (for the experimental conditions at pH 7.5). The model results suggest that the ferrihydrite surface approaches saturation with respect to sulfide at concentrations of approximately 350  $\mu M$  or above. These model results are generally consistent

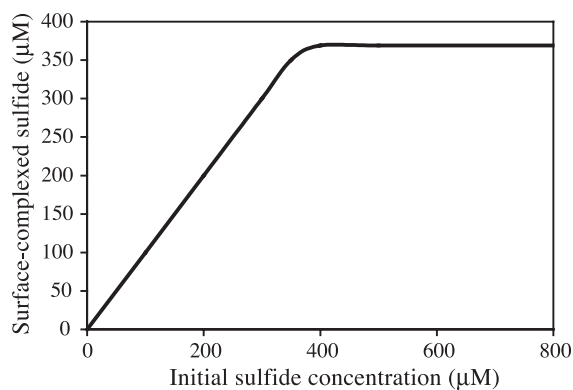


Fig. 10. Equilibrium concentrations of surface-complexed sulfide as a function of initial sulfide concentration. Concentrations were calculated using the surface complexation model, based on a ferrihydrite surface area of 100  $m^2$  in seawater at pH 7.5.

with the experimentally determined effect of initial sulfide concentration on reaction rates (Fig. 8), in that the availability of reactive surface sites may clearly inhibit reaction rates as sulfide concentrations increase. However, Fig. 10 also shows limitations in the application of surface complexation modeling to studies of reaction pathways. The surface complexation model assumes that the oxide surface is in equilibrium with respect to complexed sulfide. This is not the case experimentally because oxide surfaces do not instantaneously reach equilibrium with respect to adsorbed species (e.g. Zhang et al., 1992). Thus, the experimental data show a gradual decrease in reaction rates as dissolved sulfide increases (Fig. 8), whereas the model data show a maximum equilibrium concentration of complexed sulfide at approximately 350  $\mu\text{M}$ . Furthermore, estimates of surface-complexed sulfide in each experiment show a first order relationship with respect to reaction rates (Fig. 11), in agreement with a surface complexation control for the dissolution of iron (oxyhydr)oxides by a range of reductants (e.g. Banwart et al., 1989; Dos Santos Afonso et al., 1990; Suter et al., 1991; Dos Santos Afonso and Stumm, 1992).

The above discussion allows the contrasting observations on the relationship between total dissolved sulfide and reaction rates to be reconciled. Peiffer et al. (1992) and Yao and Millero (1996) examined the kinetics of sulfide oxidation by iron oxides at relatively low dissolved sulfide concentrations ( $\leq 100 \mu\text{M}$ ). Under these conditions, the

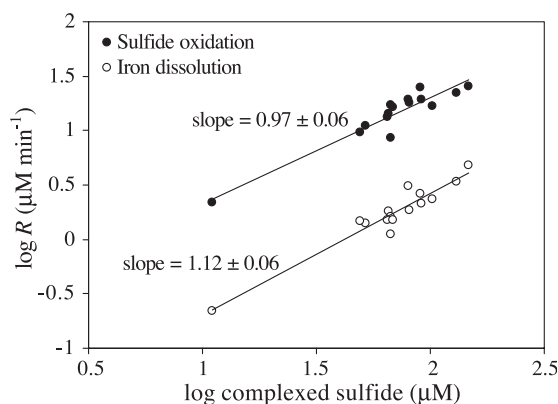


Fig. 11. Plots of reaction rate ( $R$ ) vs. estimated (see text for details) surface-complexed sulfide at pH 7.5.

availability of reactive surface sites was apparently not limiting. Thus, variations in the initial dissolved sulfide concentration are directly related to the concentration of surface-complexed sulfide. In the present study (and in the studies of Pyzik and Sommer, 1981; Canfield and Berner, 1987), the experiments were performed over a wider range of initial dissolved sulfide concentrations (150–1200  $\mu\text{M}$ ), consistent with the more variable concentrations commonly found in sulfidic sediment porewaters and euxinic basins (e.g. Brewer and Spencer, 1974; Canfield, 1989). Under these conditions, reaction rates are limited by the availability of reactive surface sites at higher concentrations of dissolved sulfide. In many natural sulfidic environments, the iron oxide to dissolved sulfide ratio is expected to be lower than during this and previous laboratory studies. Thus, surface saturation will exert an important influence on the reactivity of iron (oxyhydr)oxides in nature.

#### 4.2. Effect of pH and inhibition by seawater ions

The pronounced pH maxima observed for the reaction of ferrihydrite with dissolved sulfide (Fig. 7) is consistent with previous studies of sulfide oxidation by iron oxides (e.g. Peiffer et al., 1992; Yao and Millero, 1996), and has been observed for the dissolution of iron oxides by reductants other than sulfide (e.g. Borghi et al., 1991; Suter et al., 1991). It is well-established that the pH dependency of reaction rate occurs due to the formation of different surface species and due to changes in the speciation of the dissolved reactant. The results from this study suggest that reaction rates maximize around pH 5.5–6 (Fig. 7) where surface-protonated sites (i.e.  $>\text{FeOH}_2^+$ ) dominate the uncomplexed oxide surface (see Dos Santos Afonso and Stumm, 1992). Surface protonation accelerates the reductive dissolution of iron oxides by causing a polarization and weakening of the metal-oxygen bonds (Zinder et al., 1986; Suter et al., 1991). The speciation of dissolved sulfide is an additional consideration to reaction rates. Molecular orbital theory suggests that the sulfide species display increasing stability in the order  $\text{S}^{2-} > \text{HS}^- > \text{H}_2\text{S}$  (based on the energies of the highest occupied molecular orbital; Luther, 1990). The  $\text{S}^{2-}$  ion can be discounted at the pH of these experiments. Thus, as observed in

Table 3  
Equilibrium distributions (in %) of model surface complexes in seawater (for  $100 \text{ m}^2 \text{ l}^{-1}$  ferrihydrite in the absence of sulfide)

Species	pH 4.0	pH 6.0	pH 7.5	pH 8.5
$>\text{FeSO}_4^-$	9.0	5.2	0.7	0.03
$>\text{FeOHSO}_4^-$	0.06	2.8	14.1	9.6
$>\text{FeOHCa}^{2+}$	0.04	1.4	1.9	0.6
$>\text{FeOCa}^+$			0.4	0.6
$>\text{FeOMg}^+$		0.4	42.2	59.8
$>\text{FeONa}$			0.6	1.5
$>\text{FeOH}_2\text{Cl}$	91.0	63.1	8.2	0.2

Fig. 7, reaction rates are maximized at a pH coinciding with a high degree of surface protonation and the presence in solution of significant concentrations of the  $\text{HS}^-$  ion.

Fig. 7 also suggests that the pH dependency on reaction rates may be modified by the presence of certain inorganic solutes. The data suggest that during competition for surface sites, reaction rates are unaffected by major seawater ions at pH 7.5 and above. These results differ to those determined for hydrous ferric oxide with seawater ions pre-adsorbed, whereby reaction rates were significantly reduced by adsorbed seawater ions at pH 7.5 (Yao and Millero, 1996). Table 3 shows model equilibrium concentrations of complexes formed at the ferrihydrite surface in seawater. At pH 7.5 and above, the major surface species in seawater (discounting  $>\text{FeONa}$  and  $>\text{FeOH}_2\text{Cl}$ , which also form in the experiments performed in NaCl) decrease in the order  $>\text{FeOMg}^+$ ,  $>\text{FeOHSO}_4^-$ ,  $>\text{FeOHCa}^{2+}$ ,  $>\text{FeOCa}^+$ . The adsorption of cations and the possible outer sphere adsorption of sulfate (i.e.  $>\text{FeOHSO}_4^-$ ; see below) would be expected to decrease reaction rates due to the blocking of surface groups and the enhancement of surface deprotonation (Biber et al., 1994). The apparent inability of the major seawater ions to inhibit reaction rates at pH 7.5 and above suggests that dissolved sulfide can effectively out-compete these ions for reactive surface sites.

Poulton et al. (2003) found that, under flow-through conditions with a constant background concentration of dissolved phosphate ( $300 \mu\text{M}$ ), the pre-adsorption of phosphate to ferrihydrite significantly inhibited the initial stages of the reaction with dissolved sulfide. However, reaction rates were found to increase after the initial reaction, due to the release of surface-bound phosphate to solution during dissolu-

tion of the oxide surface. Under these conditions, reaction rates remained slower than during the flow-through of phosphate-free seawater, due to the effect of competitive adsorption. In addition, the uptake of phosphate into the oxide crystal structure during the formation of iron (oxyhydr)oxides has been shown to have no effect on reaction rates (Yao and Millero, 1996). Thus, in terms of natural sulfidic environments, competitive adsorption may ultimately have greater significance for the bulk dissolution of iron (oxyhydr)oxides, relative to either the pre-adsorption of solutes at the oxide surface or co-precipitation within the crystal structure.

The model results suggest that the decrease in reaction rates for seawater relative to NaCl under more acidic conditions (Fig. 7) may be attributable to the formation of the  $>\text{FeSO}_4^-$  surface complex (Table 3). The coordination chemistry of sulfate (i.e. inner sphere vs. outer sphere complexation) has been the subject of some discussion. However, Eggleston et al. (1998) present evidence supporting the formation of inner sphere sulfate complexes, while other studies additionally suggest the formation of binuclear sulfate complexes (Sigg and Stumm, 1981; Biber et al., 1994). Binuclear surface complexes may be particularly effective inhibitors due the increased energy required to simultaneously remove two centre atoms from the crystal lattice (Bondietti et al., 1993). The effect of sulfate on the rate of Fe(II) dissolution is shown for experimental data in Fig. 12 (a similar

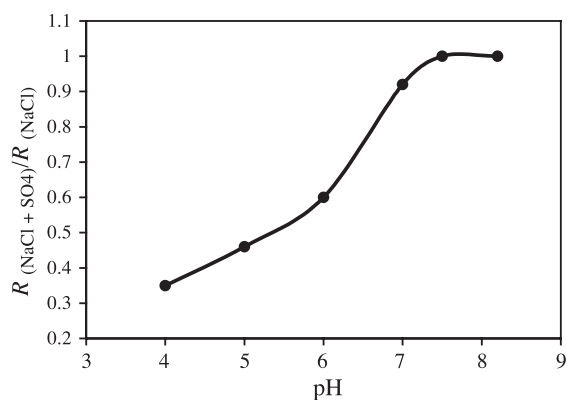


Fig. 12. Plot of the measured decrease in reaction rates due to surface-complexed sulfate as a function of pH;  $R_{(\text{NaCl} + \text{SO}_4)}$  = rate in 0.42 M NaCl with 28.9 mM dissolved sulfate;  $R_{(\text{NaCl})}$  = rate in 0.42 M NaCl.

trend was observed for the oxidation of sulfide). Consistent with the model results (Table 3), the adsorption of sulfate accounted for 98–100% of the observed reduction in reaction rates over the experimental pH range, with rates decreased by approximately 65% at pH 4.0.

## 5. Conclusion

The combined evaluation of Fe(II) dissolution and sulfide oxidation kinetics suggests that the reductive dissolution of ferrihydrite by dissolved sulfide is approximately 15 times slower than the rate of sulfide oxidation at pH 7.5. Experimental data on rates of sulfide oxidation have widely been used to evaluate the reactivity of iron minerals in terms of Fe(II) dissolution (e.g. Canfield et al., 1992). This study suggests that present reaction schemes for the sulfidation of iron (oxyhydr)oxides, which are based on a mixture of sulfide oxidation and Fe(II) dissolution data, require re-evaluation.

The reaction between dissolved sulfide and iron (oxyhydr)oxides is controlled by the formation of surface sulfide complexes and the availability of reactive surface sites. The determination of a fractional order dependence of reaction kinetics on dissolved sulfide concentration occurs due to saturation of the oxide surface at higher concentrations of dissolved sulfide. The range of initial dissolved sulfide concentrations (150–1200  $\mu\text{M}$ ) used in the present study are realistic in terms of the concentrations of sulfide commonly found in organic-rich marine porewaters and euxinic basins. However, concentrations of iron (oxyhydr)oxides will generally be considerably lower in the environment, relative to those of these experiments. Thus, surface saturation may exert an important influence on reaction kinetics in nature.

The competitive adsorption of seawater solutes has little effect on reaction rates at pH 7.5 and above. However, the inhibition of reaction rates due to sulfate adsorption under near neutral to acidic conditions may exert an important influence on the cycling of iron (oxyhydr)oxides and associated trace metals in acidic lake sediments (e.g. White et al., 1989), and in environments affected by acid mine drainage (e.g. Machemer et al., 1993).

## Acknowledgements

This study was carried out with financial support from the Commission of the European Communities, Agriculture and Fisheries (FAIR) specific RTD programme, CT98-4160 ‘Development of recirculating mariculture production systems designed to minimize environmental impact’. Michael Krom and Simon Bottrell provided helpful comments on early versions of the manuscript. Martin Schoonen, Stefan Peiffer and Eric Oelkers are thanked for constructive reviews. [EO]

## References

- Banwart, S., Davies, S., Stumm, W., 1989. The role of oxalate in accelerating the reductive dissolution of hematite ( $\alpha\text{-Fe}_2\text{O}_3$ ) by ascorbate. *Colloids Surf.* 39, 303–309.
- Bartlett, J.K., Skoog, D.A., 1954. Colorimetric determination of elemental sulfur in hydrocarbons. *Anal. Chem.* 26, 1008–1011.
- Berner, R.A., 1964. Iron sulfides formed from aqueous solution at low temperatures and atmospheric pressure. *J. Geol.* 72, 293–306.
- Biber, M.V., Dos Santos Afonso, M., Stumm, W., 1994. The coordination chemistry of weathering: IV. Inhibition of the dissolution of oxide minerals. *Geochim. Cosmochim. Acta* 58, 1999–2010.
- Bondietti, G., Sinniger, J., Stumm, W., 1993. The reactivity of Fe(III) (hydr)oxides: effects of ligands in inhibiting the dissolution. *Colloids Surf.* 79, 157–174.
- Borghi, E.B., Morando, P.J., Blesa, M.A., 1991. Dissolution of magnetite by mercaptocarboxylic acids. *Langmuir* 7, 1652–1659.
- Brewer, P.G., Spencer, D.W., 1974. Distribution of some trace elements in the Black Sea and their flux between dissolved and particulate phases. In: Degens, E.T., Ross, D.A. (Eds.), *The Black Sea-Geology, Chemistry and Biology*. AAPG, Tulsa, OK, pp. 2483–2490.
- Canfield, D.E., 1989. Reactive iron in marine sediments. *Geochim. Cosmochim. Acta* 53, 619–632.
- Canfield, D.E., Berner, R.A., 1987. Dissolution and pyritization of magnetite in anoxic marine sediments. *Geochim. Cosmochim. Acta* 51, 645–659.
- Canfield, D.E., Raiswell, R., Bottrell, S., 1992. The reactivity of sedimentary iron minerals toward sulfide. *Am. J. Sci.* 292, 659–683.
- Chen, K.Y., Morris, J.C., 1972. Kinetics of oxidation of aqueous sulfide by  $\text{O}_2$ . *Environ. Sci. Technol.* 6, 529–537.
- Cline, J.D., 1969. Spectrophotometric determination of hydrogen sulfide in natural waters. *Limnol. Oceanogr.* 14, 454–458.
- Davison, W., 1980. A critical comparison of the measured solubilities of ferrous sulphide in natural waters. *Geochim. Cosmochim. Acta* 44, 803–808.
- Davison, W., Phillips, N., Tabner, B.J., 1999. Soluble iron sulfide

- species in natural waters: reappraisal of their stoichiometry and stability constants. *Aquat. Sci.* 61, 23–43.
- Dos Santos Afonso, M., Stumm, W., 1992. Reductive dissolution of iron(III) (hydr)oxides by hydrogen sulfide. *Langmuir* 8, 1671–1675.
- Dos Santos Afonso, M., Morando, P.J., Blesa, M.A., Banwart, S., Stumm, W., 1990. The reductive dissolution of iron oxides by ascorbate. *J. Colloid Int. Sci.* 138, 74–82.
- Dzombak, D.A., Morel, F.M.M., 1990. *Surface Complexation Modeling: Hydrous Ferric Oxide*. Wiley, New York.
- Eggleston, C.M., Hug, S., Stumm, W., Sulzberger, B., Dos Santos Afonso, M., 1998. Surface complexation of sulfate by hematite surfaces: FTIR and STM observations. *Geochim. Cosmochim. Acta* 62, 585–593.
- Fredrickson, J.K., Zachara, J.M., Kennedy, D.W., Dong, H., Onstott, T.C., Hinman, N.W., Li, S.-M., 1998. Biogenic iron mineralization accompanying the dissimilatory reduction of hydrous ferric oxide by a groundwater bacterium. *Geochim. Cosmochim. Acta* 62, 3239–3257.
- Hering, J.G., Stumm, W., 1990. Oxidative and reductive dissolution of minerals. In: Hochella, M.F., White, A.F. (Eds.), *Mineral–Water Interface Geochemistry*. *Rev. Mineral.*, vol. 23, pp. 427–465.
- Heron, G., Crouzet, C., Bourg, A.C.M., Christensen, T.H., 1994. Speciation of Fe(II) and Fe(III) in contaminated aquifer sediments using chemical extraction techniques. *Environ. Sci. Technol.* 28, 1698–1705.
- Kostka, J.E., Luther III, G.W. 1995. Seasonal cycling of Fe in salt marsh sediments. *Biogeochemistry* 29, 159–181.
- Krom, M.D., Mortimer, R.J.G., Poulton, S.W., Hayes, P., Davies, I.M., Davison, W., Zhang, H., 2002. In-situ determination of dissolved iron production in recent marine sediments. *Aquat. Sci.* 64, 282–291.
- Lovely, D.R., Phillips, E.J.P., 1987. Rapid assay for microbially reducible ferric iron in aquatic sediments. *Appl. Environ. Microbiol.* 53, 1536–1540.
- Luther III, G.W., 1985. Polarographic analysis of sulfur species in marine porewaters. *Limnol. Oceanogr.* 30, 727–736.
- Luther III, G.W., 1990. The frontier-molecular-orbital theory approach in geochemical processes. In: Stumm, W. (Ed.), *Aquatic Chemical Kinetics*. Wiley, New York, NY, pp. 173–198.
- Luther III, G.W., Rickard, D.T., Theberge, S.M., Oldroyd, A., 1996. Determination of metal (bi)sulfide stability constants of  $Mn^{2+}$ ,  $Fe^{2+}$ ,  $CO^{2+}$ ,  $Ni^{2+}$ ,  $Cu^{2+}$  and  $Zn^{2+}$  by voltammetric methods. *Environ. Sci. Technol.* 30, 671–679.
- Luther III, G.W., Rozan, T.F., Taillefert, M., Nuzzio, D.B., Meo, C.D., Shank, T.M., Lutz, R.A., Cary, S.C., 2001. Chemical speciation drives hydrothermal vent ecology. *Nature* 410, 813–816.
- Machemer, S.D., Reynolds, J.S., Laudon, L.S., Wildeman, T.R., 1993. Balance of S in a constructed wetland built to treat acid mine drainage. *Appl. Geochem.* 8, 587–603.
- Mather, S.S., 1995. Development of a database for ion sorption on goethite using surface complexation modeling. MS Thesis, Carnegie Mellon University, Pittsburgh, PA, USA.
- Millero, F.J., 1986. The pH of estuarine waters. *Limnol. Oceanogr.* 31, 839–847.
- Millero, F.J., Plese, T., Fernandez, M., 1988. The dissociation of hydrogen sulfide in seawater. *Limnol. Oceanogr.* 33, 269–274.
- O'Brien, D.J., Birkner, F.B., 1977. Kinetics of oxygenation of reduced sulfur species in aqueous solution. *Environ. Sci. Technol.* 11, 1114–1120.
- Parkhurst, D.L., Appelo, C.A.J., 1999. *User's guide to PHREEQC (version 2)—a computer program for speciation, batch-reaction, one-dimensional transport, and inverse geochemical calculations*. Water-Resources Investigations Report 99-4259, Denver, CO, p. 312.
- Peiffer, S., dos Santos Afonso, M., Wehrll, B., Gachter, R., 1992. Kinetics and mechanism of the reaction of  $H_2S$  with lepidocrocite. *Environ. Sci. Technol.* 26, 2408–2413.
- Poulton, S.W., Raiswell, R., 2000. Solid phase associations, oceanic fluxes and the anthropogenic perturbation of transition metals in world river particulates. *Mar. Chem.* 72, 17–31.
- Poulton, S.W., Raiswell, R., 2002. The low-temperature geochemical cycle of iron: from continental fluxes to marine sediment deposition. *Am. J. Sci.* 302, 774–805.
- Poulton, S.W., Krom, M.D., van Rijn, J., Raiswell, R., 2002. The use of hydrous iron(III) oxides for the removal of hydrogen sulphide in aqueous systems. *Water Res.* 36, 825–834.
- Poulton, S.W., Krom, M.D., van Rijn, J., Raiswell, R., Bows, R., 2003. Detection and removal of dissolved hydrogen sulphide in flow-through systems via the sulphidation of hydrous iron(III) oxides. *Environ. Technol.* 24, 217–229.
- Pyzik, A.J., Sommer, S.E., 1981. Sedimentary iron monosulfides: kinetics and mechanism of formation. *Geochim. Cosmochim. Acta* 45, 687–698.
- Rickard, D.T., 1974. Kinetics and mechanism of the sulfidation of goethite. *Am. J. Sci.* 274, 941–952.
- Rickard, D., Oldroyd, A., Cramp, A., 1999. Volumetric evidence for soluble FeS complexes in anoxic estuarine muds. *Estuaries* 22, 693–701.
- Salomons, W., Forstner, U., 1984. *Metals in the Hydrocycle*. Springer-Verlag, Berlin, pp. 215–257.
- Schwertmann, U., Cornell, R.M., 1991. *Iron Oxides in the Laboratory: Preparation and Characterisation* Weinheim, Cambridge.
- Sigg, L., Stumm, W., 1981. The interactions of anions and weak acids with the hydrous goethite surface. *Colloids Surf.* 2, 101–117.
- Stookey, L.L., 1970. Ferrozine—a new spectrophotometric reagent for iron. *Anal. Chem.* 42, 779–781.
- Stumm, W., Wieland, E., 1990. Dissolution of oxide and silicate minerals: rates depend on surface speciation. In: Stumm, W. (Ed.), *Aquatic Chemical Kinetics*. Wiley, New York, NY, pp. 367–400.
- Suter, D., Banwart, S., Stumm, W., 1991. Dissolution of hydrous iron(III) oxides by reductive mechanisms. *Langmuir* 7, 809–813.
- Theberge, S.M., Luther III, G.W. 1997. Determination of the electrochemical properties of a soluble aqueous FeS species present in sulfidic solutions. *Aquat. Geochem.* 3, 191–211.
- Tippling, E., 1981. The adsorption of aquatic humic substances by iron oxides. *Geochim. Cosmochim. Acta* 45, 191–199.
- Urban, P.J., 1961. Colorimetry of sulphur anions: I. An improved colorimetric method for the determination of thiosulphate. *Z. Anal. Chem.* 179, 415–422.

- Viollier, E., Inglett, P.W., Hunter, K., Roychoudhury, A.N., Van Cappellen, P., 2000. The ferrozine method revisited: Fe(II)/Fe(III) determination in natural waters. *Appl. Geochem.* 15, 785–790.
- West, P.W., Gaeke, G.C., 1956. Fixation of sulfur dioxide as disulfidomercurate(II) and subsequent colorimetric estimation. *Anal. Chem.* 28, 1816–1819.
- White, J.R., Gubala, C.P., Fry, B., Owen, J., Mitchell, M.J., 1989. Sediment biogeochemistry of iron and sulfur in an acidic lake. *Geochim. Cosmochim. Acta* 53, 2547–2559.
- Yao, W., Millero, F.J., 1996. Oxidation of hydrogen sulfide by hydrous Fe(III) oxides in seawater. *Mar. Chem.* 52, 1–16.
- Zhang, J., Millero, F.J., 1994. Investigation of metal sulfide complexes in seawater using cathodic stripping square wave voltammetry. *Anal. Chim. Acta* 284, 497–504.
- Zhang, J., Charlet, L., Schindler, P.W., 1992. Adsorption of protons, Fe(II) and Al(III) on lepidocrocite ( $\gamma$ -FeOOH). *Colloids Surf.* 63, 259–268.
- Zinder, B., Furrer, G., Stumm, W., 1986. The coordination chemistry of weathering: II. Dissolution of Fe(III) oxides. *Geochim. Cosmochim. Acta* 50, 1861–1869.